Molecular Docking & MD Simulation Studies to Design Benzothiazole-Thiazole Hybrids as Potent p56lck Inhibitors for the Treatment of Cancer

Payal Jain [1,2], Malleshappa N. Noolvi [2,*] ⓘ, Uttam A. More [2,*], Mahesh B. Palkar [3]

[1]   Pharmacy, Gujarat Technological University, Ahmedabad, India
[2]   Department of Pharmaceutical Chemistry, Shree Dhanvantary Pharmacy College, Kim, Surat 394110, Gujarat, India
[3]   Department of Pharmaceutical Chemistry, Shobhaben Pratapbhai Patel School of Pharmacy Technology Management SVKM's Narsee Monjee Institute of Management Studies University (NMIMS), Vile Parle (W), Mumbai, 400 056, Maharashtra, India
*   Correspondence: noolvimalleshappa@gmail.com;

Abstract: The p56^{lck} enzyme is mainly known for its important role in T cells. Immense effort has been put into developing p56^{lck} inhibitors for diseases such as cancer, osteoporosis, and many others. Various studies on benzothiazole derivatives are of great interest because of their potent antitumor activity, and they act by binding to the ATP binding site of protein kinase. The protein kinase ATP binding site provided a great opportunity to develop newer analogs for protein kinase inhibitors. In the present investigation, we carried out ADMET molecular docking and Molecular Dynamic Simulation to know the structural requirements for inhibition of the p56^{lck} enzyme. A docking study was performed on 51 analogs of benzothiazole and MD Simulation on three selected molecules. A molecular docking study on designed molecules and some standard molecules gives information on binding patterns like hing region, Allosteric site, and activation loop. ADMET study results allowed us to determine the selectivity of substitution and to know whether molecules obey Lipinski's rule of five or not. Compound **1** was identified as a competitive inhibitor of p56^{lck} by Molecular docking and MD Simulation. The benzothiazole-thiazole hybrids revealed structural features required to inhibit p56^{lck}.

Keywords: benzothiazole-thiazole derivatives; molecular docking; molecular dynamic simulation; anticancer agents.

1. Introduction

Cancer is 2nd leading cause of death and an important barrier to increasing life expectancy in the world. Cancer is the leading cause of death across 112 of 183 countries, according to the WHO 2019 report. The number of new cancer cases diagnosed in 2020 was 19.3 million, and around 10.0 million died because of cancer, as per GLOBOCAN 2020 report. The number of cancer cases will rise to 28.4 million by 2040, as per GLOBOCAN prediction. As per cancer mortality, lung cancer is the leading cause, responsible for 1.8 million deaths (18%), then colorectal (9.4%), liver (8.3%), stomach (7.7%), and female breast cancer (6.9%). The main leading types of cancer among men are lung, prostate, and colorectal, whereas in women, breast,

colorectal, and lung are the leading cancers. Cancer is 5th leading cause of death, around 5.7% of all deaths in India, as per the 2018 report of The Medical Certification of Cause of Death. The 0.8 million new cancer cases rise every year reported by the cancer burden [1-5].

Cancer treatment has become an important and challenging therapeutic task in medicinal chemistry. Three main 3 treatment strategies emerged: radiation therapy, surgery, and chemotherapy. Treatment of cancer is usually a combination of several different techniques. If the tumor is curable, then surgery is the single most effective technique. One of the best cancer treatments is chemotherapy, but it is associated with various side effects. So, it is a challenge to discover potent antitumor agents without side effects to develop new cancer chemotherapeutic agents in the future [6, 7].

Protein tyrosine kinases (PTKs) are involved in signaling pathways and regulate cell activation, growth, transformation, and differentiation. Malfunctions of cellular signaling have been related to several diseases, including diabetes and cancer. Protein tyrosine kinases are divided into two types: (i) Receptor Tyrosine Kinases (RTKs) and Non-receptor Tyrosine Kinases (NRTKs). The Src family belongs to Non-receptor tyrosine kinases, which play an important role in signal transduction. Fyn, Src, and Yes are members of the Src family, and they are found in most cell types, whereas other members like Lck, Hck, and Blk exhibit a more restricted tissue distribution, and they have an important role in signal transduction [8].

A central switching mechanism in cellular signal transduction pathways occurs by the protein tyrosine kinases by catalyzing the transfer of the γ-phosphate of either GTP or ATP to specific tyrosine residues in protein substrates [9, 10]. $p56^{lck}$ (LCK) is one of the members of the Src family, and it is expressed in natural killer cells and T-lymphocytes. $p56^{lck}$ contains a SH2 domain that participates in signaling pathways initiated through the T-cell antigen receptor on T lymphocytes. For the regulation and recruitment of $p56^{lck}$ kinase activity, the SH2 domain is responsible. $p56^{lck}$ contains 509 amino acids polypeptide chains with a molecular weight of 58.097 kDa. Lck is required for T-cell antigen receptor (TCR) signaling in T cells, culminating in IL-2 gene expression and effector functions [11-14].

For T-cell development and function, Lck is essential. It plays an important role in T-cell antigen receptor (TCR) linked signal transduction pathways and is mainly associated with the cytoplasmic portions of the CD4 and CD8 surface receptors. For TCR signaling, Lck activates and phosphorylates various substrates. LCK catalytic activity is regulated by two sites of tyrosine phosphorylation: Tyr394 in the catalytic domain and Tyr505 on the C-terminus. Through the actions of the kinase Csk and phosphatase CD45, Tyr394 is phosphorylated, and Tyr505 is dephosphorylated; the tyrosine residues within a special sequence are phosphorylated by a fully activated enzyme called the immunoreceptor tyrosine activation motif (ITAM) located on the ζ-chain of the TCR. This type of phosphorylation makes a docking site for its downstream substrate ZAP-70 binding via its SH2 domains, which must be phosphorylated by Lck to be activated. Lck's dual phosphorylation of tyrosine residues in ITAMs is required to bind tandem ZAP-70 Src homology domains. Subsequent LCK phosphorylated ZAP- 70 triggers a series of downstream cascade events that lead to mobilization of intracellular Ca^{++} and activation of protein kinase C (PKC), T cell activation, and proliferation. So, functional disorders in these cell regulatory processes may lead to diseases such as cancer, allergy, osteoporosis, inflammation, and asthma [15-23].

These types of discoveries indicate that Lck inhibitors should inhibit T cell activation, which is useful for T cell-mediated autoimmune diseases and graft rejection. Over the past decade, major pharmaceutical research has focused on developing small molecule Lck inhibitors. Recognizing Lck inhibitors is remarkably difficult due to Lck's membership in the SRC family. The Src family is highly homologous, and kinases play a crucial role in controlling a wide variety of cellular processes. The lck inhibitor is very specific towards other members of the Src family kinase with little or no activity. Due to a lack of structural information about the Src family kinase, this task was initially complicated; a significant amount of knowledge about the structural differences, similarities, and the nature of the small molecule inhibitors that show specificity within this family generated from a decade of research [15, 20].

1.1. Kinase inhibitor binding sites.

Protein kinases exhibit the ability to facilitate the transfer of the terminal phosphate from ATP to substrates, typically comprised of tyrosine, serine, and threonine residues. They commonly share a conserved organization of secondary structural elements, divided into 12 subdomains, which fold into a catalytic core structure with two lobes. The lobes enclose a deep cleft where ATP binds, with its adenine ring forming hydrogen bonds with the kinase hinge-a segment connecting the amino and carboxy-terminal kinase domains. The ribose and triphosphate moieties of ATP occupy a hydrophilic channel extending towards the substrate binding site, featuring conserved residues crucial for catalytic activity. Kinases universally possess an activation loop, crucial for regulating kinase activity, characterized by conserved DFG and APE motifs at their beginning and end, respectively.

The activation loop encompasses a wide range of conformations, from a catalytically competent form, typically phosphorylated, to an inactive state where the activation loop obstructs the substrate binding site. Primarily, kinase inhibitors, identified as ATP competitive, establish one to three hydrogen bonds with amino acids situated in the hinge region of the target kinase, thus imitating the hydrogen bonds typically formed by the adenine ring of ATP [24].

1.2. Lck inhibitors.

Identical ligands with Structural studies identify the challenge of developing Src family kinase (SFK) isoform-specific inhibitors. Crystal structures with the ATP mimetic AMP-PNP exhibit identical hydrogen binding to conserved residues of Src, Lck, and Hck [16, 20].

Thiazole and benzothiazole as modestly potent Lck inhibitors were identified by high-throughput screening of the compound [11-15]. Thiazoles were reported to exhibit antimicrobial, antibacterial, analgesic, antioxidant, anti-inflammatory, anticonvulsant, antidiabetic, insecticidal, antitubercular, antifungal, antiprotozoal, cardiotonic, herbicidal, analgesic, anthelmintic, Syk inhibitor, antiviral, neuro-protective agent and antimalarial activities [25-41]. Benzothiazole stands out as a significant compound characterized by its weak base properties and diverse biological activities, including antitumor, anti-HIV, antimicrobial, antitubercular, antifungal, antioxidant, anticonvulsant, antileishmanial, anthelmintic, diuretic, analgesic, anti-inflammatory, antipsychotic, anti-ulcer, schistosomicidal and local anesthetic [42-53].

Benzothiazole structure-activity relations and their biological activities, like p56[lck] inhibitory and antitumor activity, have been studied. As per the literature survey structure-activity study of benzothiazoles show a binding model of benzothiazole Lck inhibitors; based on published literature, the activated Lck kinase domain bound to ANP (phosphoaminophosphonic acid adenylate ester, a non-hydrolyzable ATP mimic) [10].

The researchers at BMS optimized both thiazole and benzothiazole derivatives, which were among the most potent inhibitors discovered in these studies. At C2, amino group modification also leads to potent Lck inhibitors for the class benzothiazole and thiazole [54].

Focusing on the p56[lck] SH2 domain for potential future targets and the recent advances in drug design. Many labs are working on synthesizing molecules that can bind tightly to the p56[lck] SH2 domain, hindering substrate recruitment and thereby artificially controlling its effect on T-cells to generate immunosuppressant and anticancer agents. Lck is most important for TCR singling, so the target is to inhibit the T-Cell singling pathway to develop new Lck inhibitors [14]. So many heterocyclic rings like benzothiazole, thiazole, thiadiazole, pyrimidine, and imidazoquinoxalines inhibit the T-cell singling and ultimately inhibit the Lck.

J.D. *et al*. [12] reported that substituting the 2-carboxamide group with particular heteroaryl amines in Lck inhibitors has yielded highly potent Lck inhibitors. To design a new molecule with thiazole as the core moiety, we applied both approaches. Figure 1 introduces the initial strategy for identifying fragments essential for biological activity. This approach involves analyzing pharmacophoric requirements and creating novel hybrids. These hybrids are characterized by a linkage where benzothiazole is connected to thiazole at the second position via a secondary amine, with an amide linkage at the other end. The second approach we employed is structure-based drug design. In this method, we utilized the crystalline structure of p56lck to gain mechanistic insights into how the designed molecules interact with receptors, thereby achieving improved anticancer profiles.
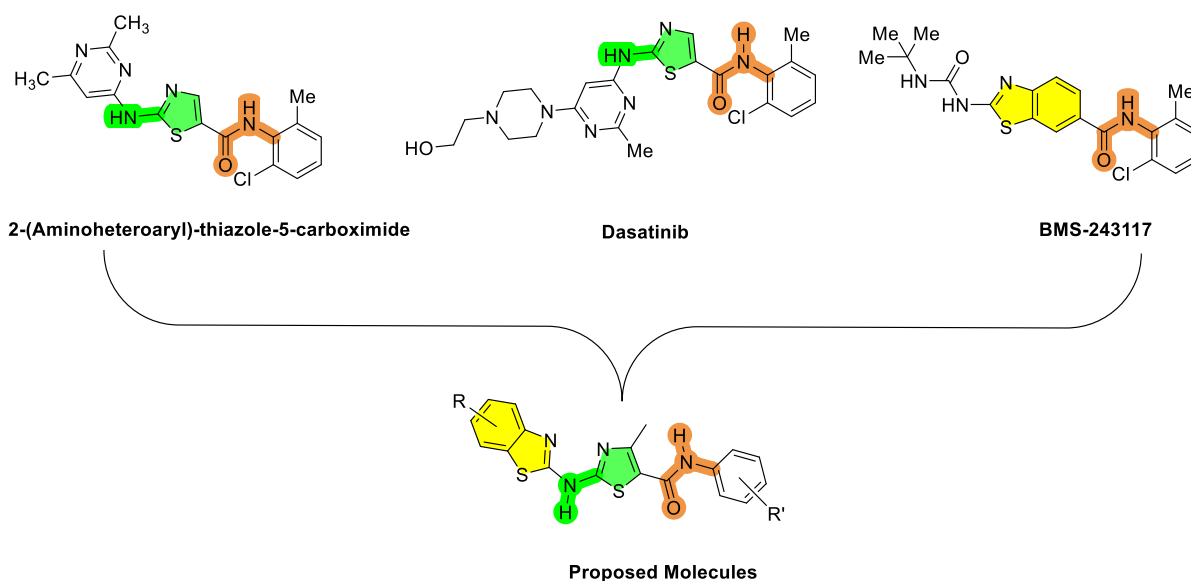
Figure 1. Designing of new benzothiazole-thiazole hybrids; **I:** 2-(Aminoheteroaryl)-thiazole-5-carboximide; **II:** Dasatinib; **III:** BMS-243117.

2. Materials and Methods

2.1. Theoretical ADME prediction.

One significant step in the drug development process is the evaluation of the pharmacokinetic properties of molecules. In silico ADME analysis can be used to identify lead molecules to check for their convenient drug-likeness and bioavailability. Nearly 40 percent of medicinal candidates miss clinical trials due to bad ADME properties (absorption, distribution, metabolism, and excretion). Drug kinetics and tissue exposure to drugs affect the pharmacological activity and the effectiveness of medicines, which is finally decided by ADME properties. Therefore, we used QikProp to predict ADME properties *in silico* for all 51 benzothiazole derivatives. Descriptors like CNS, SASA, Volume, QPlogPo/w, QPlogS, QPlogHERG, QPPCaco, QPPMDCK, QplogBB, QplogKhsa, % human oral absorption, and PSA were calculated using QikProp module (Qikprop, Schrödinger, LLC, NY, 2017).

2.2. Molecular docking.

The molecular docking software GLIDE (Schordinger Inc., USA) [55] was employed to conduct ligand docking investigations within the binding pocket of the tyrosine kinase receptor. The crystal structures of LCK were sourced from the Protein Data Bank (PDB ID: 1QPC) [16]. Protein preparation involved two steps using the protein preparation wizard in Maestro 9.0: preparation and refinement. After ensuring chemical correctness, water molecules in the crystal structures were deleted, and hydrogens were added where they were missing. Using the OPLS 2005, the force field energy of crystal structure was minimized. Grids were defined centering them on the ligand in the crystal structure using the default box size. The ligands were built using maestro build panel and prepared by the Ligprep module (LigPrep, Schrödinger, LLC, NY, USA), which produces the low energy conformer of ligands using the OPLS 2005 force field. The ligands' low energy conformation was selected and docked into the grid generated from protein structures using standard precision (SP) docking mode. The final evaluation is done with a glide score (docking score), and a single best pose is generated as the output for a particular ligand.

2.3. Molecular dynamic simulation.

The 3D structure of Lck complexed with benzothiazole analogs were used for MD simulation. *Standard Dynamics Cascade* protocol in BIOVIA® DS [56] used for MD simulation, which follows the main four steps like minimization, heating and cooling, equilibrium run, and production run, minimization of the 3D structures to find the most stable conformation of the 1QPC-benzothiazole complexes were carried out using the Steepest Descent algorithm followed by the Conjugate Gradient algorithm for 2000 steps each. After the minimization step, all complexes were subjected to gradual heating from 50K to 300K with a time interval of 2 fs. The system was stabilized at around 300K temperature in the equilibration phase. After equilibrium, 1QPC-benzothiazole complexes were subjected to the production run at constant-temperature, constant-volume ensemble (NVT) for initially 100ps. The SHAKE algorithm [57] constraint was set to true for all covalent bonds involving hydrogen atoms at their respective distances from the charmm27 force field [58] parameters.

3. Results and Discussion

3.1. ADME prediction.

Using the QikProp tool, the ADME properties of benzothiazole derivatives (1-51) were carried out. Predicted results are listed in Table 1. ADME-based analysis is an important method for analyzing the effectiveness of drug molecules. Descriptors like CNS, SASA, Volume, QPlogPo/w, QPlogS, QPlogHERG, QPPCaco, QPPMDCK, QplogBB, QplogKhsa, % human oral absorption, and PSA were calculated using this model. In the first series of compounds 1-5,7,8,10,14-16,19,21-23,25,28-30,33-34,36,38,39,42,44-48,50 and 51 showed promising CNS activity, remaining compounds showed 0,-1 and -2 CNS value. Regarding % human oral absorption, 25 compounds showed 100% absorption, 20 compounds showed >90% absorption, compounds 24 and 25 showed >80% absorption, compounds 11 and 31 showed >60% absorption, and compounds 26-27 showed >50% absorption.

3.2. Docking study.

A docking study was carried out for the target compounds using GLIDE (Schrödinger) (2006). The crystal structure of the LCK (1QPC) was obtained from the protein data bank PDB. A binding model for these benzothiazole Lck inhibitors was developed based on the published data of the activated Lck kinase domain bound to ANP (phosphoaminophosphonic acid-adenylate ester, a non-hydrolyzable ATP mimic).
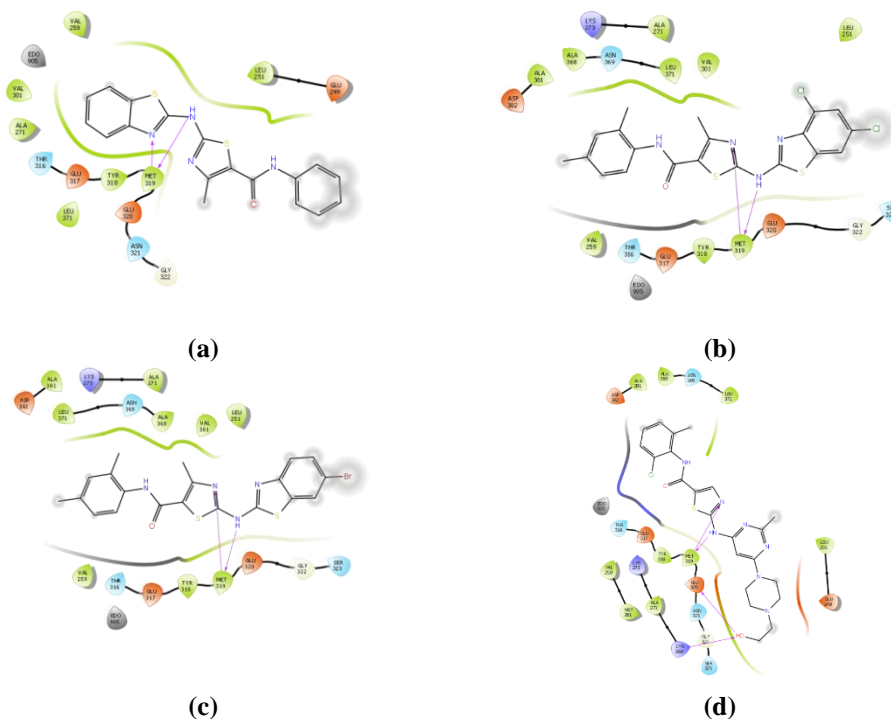
Figure 2. Proposed and Standard molecules binding mode at the ATP site of Lck **(a)** Compound 1; **(b)** Compound 2; **(c)** Compound3; **(d)** Dasatinib.

Table 1. QikProp ADMET prediction of the benzothiazole-thiazole hybrids (1-51).

Compnd.	CNS[a]	SASA[b]	Volume[c]	QPlogPo/w[d]	QPlogS[e]	QPlogHERG[f]	QPPCaco[g]	QPlogBB[h]	QPPMDCK[i]	QPlogKhsa[j]	%HOA[k]	PSA[l]	mol_MW[m]	HBD[n]	HBA[o]	#metab[p]	RO5[q]	RO3[r]
1	0	655.025	1112.054	3.955	-5.715	-6.876	2224.42	-0.186	3586.599	0.264	100	66.876	366.455	2	6	4	0	1
2	1	742.916	1304.407	5.417	-7.762	-6.238	2405.86	0.125	10000	0.756	100	64.87	463.399	2	6	5	1	1
3	0	734.645	1274.205	5.043	-7.378	-6.479	2269.971	-0.046	8600.516	0.674	100	65.565	473.404	2	6	5	1	1
4	1	692.77	1178.77	4.88	-7.134	-6.432	2267.456	0.234	10000	0.427	100	66.548	438.417	2	6	3	0	1
5	0	696.501	1249.321	4.67	-6.513	-6.007	1826.223	-0.206	3758.164	0.629	100	66.379	473.404	2	6	6	0	1
6	-1	706.435	1228.317	3.941	-6.447	-6.555	430.155	-0.884	1616.503	0.337	100	109.455	490.348	2	7	4	0	1
7	0	755.934	1335.362	5.107	-7.413	-6.194	2532.235	-0.175	3663.641	0.837	100	64.662	422.562	2	6	7	1	2
8	1	725.71	1248.623	5.445	-7.832	-6.559	2371.589	0.318	10000	0.605	93.318	66.043	514.241	2	6	3	2	1
9	-2	730.874	1268.713	4.196	-7.101	-6.457	282.256	-1.002	2043.338	0.434	95.376	111.197	480.343	2	7	4	0	1
10	1	734.181	1279.048	5.142	-7.414	-6.431	2499.11	0.032	10000	0.688	100	66.064	473.404	2	6	5	1	1
11	-2	716.544	1248.934	2.686	-5.792	-6.547	51.241	-2.204	61.101	0.164	60.313	154.453	456.45	2	8	5	1	1
12	-2	710.16	1232.766	3.781	-6.456	-6.564	284.006	-1.13	882.97	0.347	92.996	111.174	490.348	2	7	4	0	1
13	-1	667.012	1194.037	3.544	-5.524	-6.105	435.181	-0.908	775.637	0.274	94.924	109.757	490.348	2	7	5	0	0
14	1	675.605	1147.536	4.421	-6.434	-6.701	2246.948	0.011	10000	0.35	100	66.512	402.436	2	6	4	0	1
15	0	753.941	1334.665	5.059	-7.338	-6.214	2372.938	-0.228	3038.786	0.836	100	64.567	422.562	2	6	8	1	2
16	0	697.286	1246.455	4.649	-6.522	-6.042	1840.356	-0.209	3731.886	0.62	100	66.429	428.953	2	6	6	0	1
17	-2	707.663	1225.425	3.718	-6.395	-6.571	282.22	-1.145	831.381	0.328	92.574	111.203	445.897	2	7	4	0	1
18	-2	711.945	1225.293	3.707	-6.457	-6.656	283.153	-1.171	809.117	0.324	92.537	110.992	445.897	2	7	5	0	1
19	1	725.418	1297.688	5.798	-8.059	-5.906	1777.887	0.346	10000	0.748	93.146	66.557	538.68	2	6	3	2	1
20	-2	723.952	1239.073	3.825	-6.743	-6.725	264.712	-1.193	952.588	0.354	92.705	111.839	490.348	2	7	4	0	1
21	1	743.033	1331.951	5.569	-7.882	-5.884	1827.791	0.076	10000	0.836	100	66.39	497.844	2	6	5	1	1
22	1	721.3	1248.393	5.454	-7.765	-6.478	2377.757	0.333	10000	0.608	93.393	66.199	514.241	2	6	3	2	1
23	1	698.192	1205.189	4.974	-7.056	-6.592	2376.747	0.171	10000	0.499	100	66.198	479.796	2	6	3	0	1
24	-1	747.199	1305.348	4.564	-7.582	-6.355	282.837	-0.9	3657.766	0.528	84.586	111.184	514.788	2	7	4	1	1
25	1	687.994	1224.482	5.01	-6.919	-6.087	1799.87	0.097	10000	0.563	88.625	66.606	514.241	2	6	3	2	1
26	-2	733.367	1259.246	2.564	-6.074	-6.7	31.412	-2.552	35.875	0.178	55.795	156.845	456.45	2	8	5	1	1
27	-2	733.367	1259.255	2.564	-6.074	-6.7	31.417	-2.552	35.88	0.178	55.797	156.846	456.45	2	8	5	1	1
28	2	748.102	1340.458	6.254	-8.72	-5.842	1799.401	0.486	10000	0.857	95.91	66.611	573.125	2	6	3	2	1
29	1	711.352	1263.447	5.459	-7.628	-6.024	1797.822	0.249	10000	0.659	91.247	66.647	504.235	2	6	3	2	1
30	1	730.019	1290.922	5.36	-7.504	-6.245	2535.204	0.147	10000	0.725	100	64.053	463.399	2	6	6	1	1
31	-2	675.207	1214.223	2.692	-4.995	-6.085	120.442	-1.669	111.676	0.105	66.992	153.509	456.45	2	8	6	1	0
32	-2	704.206	1268.141	3.778	-5.962	-5.989	469.844	-1.019	488.276	0.455	96.889	109.992	439.506	2	7	7	0	2
33	1	687.318	1219.338	4.972	-6.902	-6.113	1796.86	0.09	10000	0.549	100	66.64	469.79	2	6	4	0	1
34	0	662.637	1174.518	4.476	-6.162	-6.191	1788.283	-0.073	7108.785	0.439	100	66.621	435.345	2	6	4	0	1
35	-2	715.407	1233.091	3.77	-6.534	-6.662	283.683	-1.162	853.486	0.343	92.923	111.003	490.348	2	7	5	0	1
36	1	708.733	1261.073	5.413	-7.535	-6.034	1799.802	0.226	10000	0.654	90.988	66.626	504.235	2	6	4	2	1
37	-1	691.697	1234.806	3.992	-6.248	-6.062	423.175	-0.788	1838.095	0.369	100	109.825	480.343	2	7	5	0	1
38	0	661.609	1177.416	4.488	-6.139	-6.148	1772.846	-0.075	6935.106	0.448	100	66.57	479.796	2	6	4	0	1
39	1	684.648	1220.539	4.966	-6.843	-6.053	1773.025	0.083	10000	0.554	100	66.575	514.241	2	6	4	1	1
40	-1	669.686	1201.659	3.631	-5.598	-6.094	457.7	-0.868	890.716	0.293	95.822	110.138	490.348	2	7	5	0	0

Table 1. QikProp ADMET prediction of the benzothiazole-thiazole hybrids (1-51).
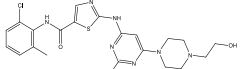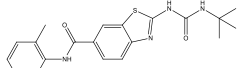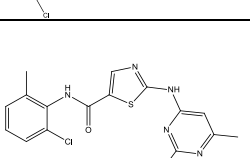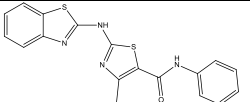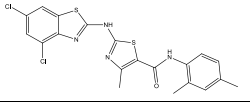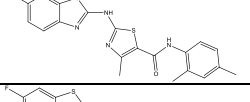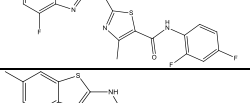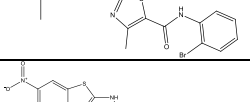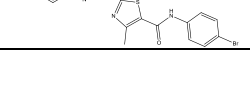
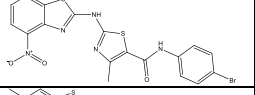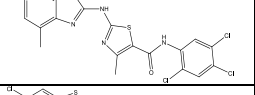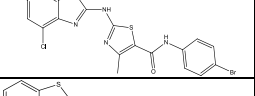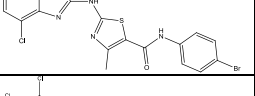| Compnd.	CNS[a]	SASA[b]	Volume[c]	QPlogPo/w[d]	QPlogS[e]	QPlogHERG[f]	QPPCaco[g]	QPlogBB[h]	QPPMDCK[i]	QPlogKhsa[j]	%HOA[k]	PSA[l]	mol_MW[m]	HBD[n]	HBA[o]	#metab[p]	RO5[q]	RO3[r]
41	-1	667.542	1191.199	3.506	-5.526	-6.138	417.551	-0.938	726.727	0.265	94.38	109.808	445.897	2	7	5	0	0
42	0	661.207	1180.877	4.513	-6.135	-6.11	1774.693	-0.069	6988.863	0.458	100	66.528	524.247	2	6	4	1	1
43	-1	692.536	1241.457	4.056	-6.276	-6.026	436.122	-0.759	1978.441	0.388	100	110.061	480.343	2	7	5	0	1
44	1	709.679	1261.729	5.44	-7.59	-6.006	1788.057	0.243	10000	0.655	91.091	66.614	504.235	2	6	4	2	1
45	0	721.238	1290.452	5.135	-7.247	-5.953	1838.389	-0.051	9189.138	0.73	100	66.437	463.399	2	6	5	1	1
46	1	700.036	1211.956	5.034	-7.106	-6.574	2388.94	0.186	10000	0.518	90.966	66.172	524.247	2	6	3	2	1
47	1	717.971	1229.288	5.323	-7.749	-6.448	2223.447	0.314	10000	0.555	100	66.919	471.326	2	6	3	1	1
48	0	742.986	1312.252	5.224	-7.459	-6.222	2514.766	-0.018	7981.872	0.778	100	64.3	442.98	2	6	7	1	2
49	-1	669.77	1198.017	3.582	-5.589	-6.124	435.668	-0.903	818.686	0.283	95.155	110.167	445.897	2	7	5	0	0
50	0	662.195	1178.365	4.501	-6.156	-6.149	1784.484	-0.069	7126.244	0.45	100	66.578	479.796	2	6	4	0	1
51	1	712.143	1217.605	5.075	-7.366	-6.709	2238.146	0.161	10000	0.525	90.703	66.858	524.247	2	6	3	2	1
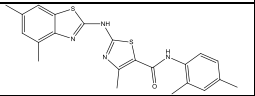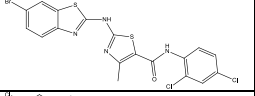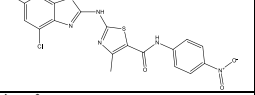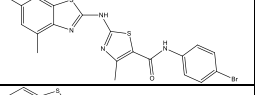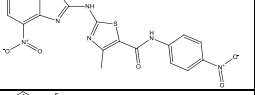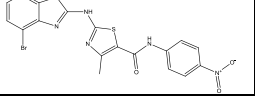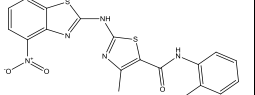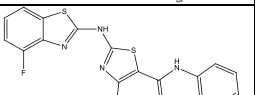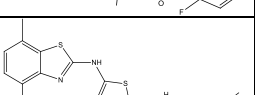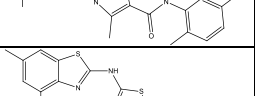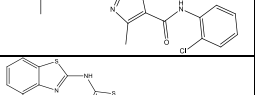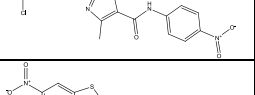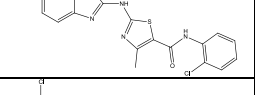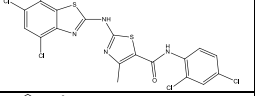
[1]Table: [a]CNS:- Central Nervous System, Predicted value (i) active scale (+2) (ii) inactive scale (-2); [b]SASA:- Solvent Accessible Surface Area used a probed with 1.4 °A radius (300 to 1000); [c]Volume:- Total solvent-accessible volume used a probe with1.4 °A radius (500 to 2000) [d]QPlog Po/w:- Partition coefficient of octanol/water, Predicated value: -2.0 to -6.5; [e]QPlogS:- Aqueous Solubility in mol dm^{-3}, Predicated value: -6.5 to -0.5; [f]QPlogHerg:- Blockage of HERG K$^+$ channels; Predicated IC50 value: > -5; [g]QPPCaco:- Gut-blood barrier in nm/sec; Predicated value for non active transport (poor: <25 and great: >500); [h]QPlogBB:- Brain/Blood partition coefficient; [j]QPlogKhsa:- Binding to human serum albumin, Predicated value: (-1.5 -1.5); [i]QPPMDCK:- MDCK cell permeability in nm/second, Predicated value for non active transport (poor: <25 and great: >500); [k]%Human Oral Absorption:- Predicated value: (poor: <25% and high: >80%); [l]PSA:- Polar Surface Area; [m]Mol MW:- Molecular Weight of molecule, Predicated value: (130.5 to 725.0); [n]donorHB:- No. of hydrogen bond donor, Predicated value: (0.0 to 6.0); [o]accptHB:- No. of hydrogen bond acceptor, Predicated value: (2.0 to 20.0); [p]#metab:- No. of metabolic reaction, Predicated value: (1 to 8); [q]Rule of Five (Lipinski's Rule):- (i) molecular weight is <500; (ii) QlogPo/w is <5, (iii) donorHB is ≤ 5 (iv) accptHB is ≤ 10; [r]Rule of Three:- (i) QPlogS is > -5.7 (ii) QPPCaCo is >22 nm/s, #primary Meabolites is <7.
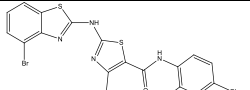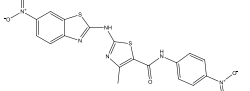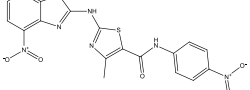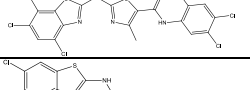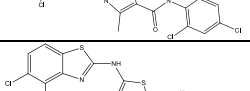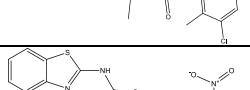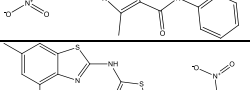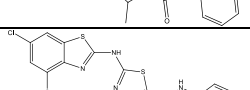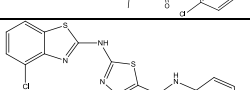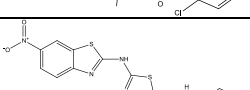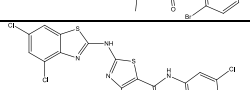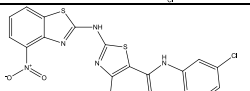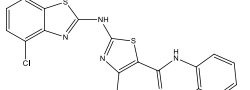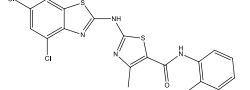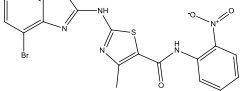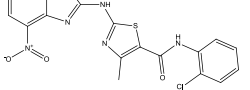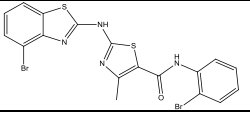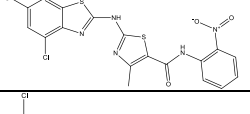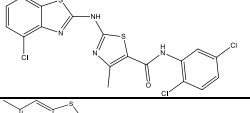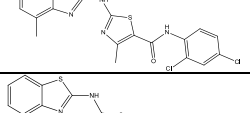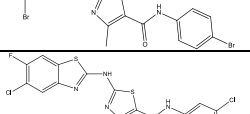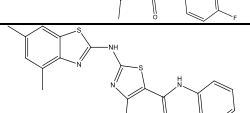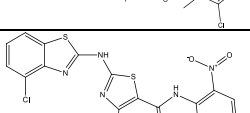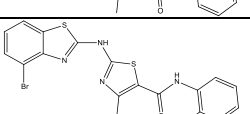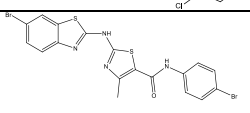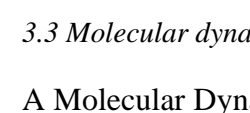
As shown in Figure 2, compound 1 binds in an extended conformation to the ATP-binding site of Lck. The entire complex was then subjected to alternate cycles of minimization and dynamics. The intent was to get a satisfactory complex structure consistent with the published crystal structure. From the comparative docking study of our compounds with standard molecules such as dasatinib, BMS 243117, and 2-(Aminoheteroaryl)-thiazole-5-carboximide we could observe how our compounds might bind to the kinase binding site, based on the knowledge of the structure of similar active sites. The substituted aniline ring is out of plane concerning the benzothiazole core, which, in turn, allows the phenyl ring to fit into the narrow and angular hydrophobic pocket. These docking studies have revealed that the nitrogen of benzothiazole moiety makes a hydrogen bond with the backbone of carbonyl of (H) MET319 in the hydrophobic pocket. At the same time, secondary amine also forms a hydrogen bond with the backbone of carbonyl of with the same amino acid (O) MET319 in a hydrophobic pocket. These interactions underscore the importance of both nitrogen atoms for binding and the subsequent inhibitory capacity. The docking score of all 51 compounds and standard compounds is mentioned in Table 2. For the inhibition action of Lck, the necessary thing is an analog of benzothiazole, and thiazole fits into a narrow and angular hydrophobic pocket and makes hydrogen bonding with a backbone of carbonyl of an amino acid (Figure 2). It makes a similar type of interaction to standard molecules Dasatinib.

Table 2. Docking score for benzothiazole-thiazole hybrids and standard compounds.

No.	Compound	Docking score (kcal/mol)	Glide lipo	Glide H bond interaction	Glide evdw interaction	Glide ecoul	Glide E-model	Glide Energy (kcal/mol)
Dasatinib		-7.379	-2.328	-0.242	-47.138	-9.738	-73.375	-56.876
BMS-243117		-6.732	-2.665	-0.46	-37.547	-8.616	-63.229	-46.163
2-(Aminoheteroaryl)-thiazole-5-carboximide		-6.52	-2.456	-0.018	-41.823	-3.687	-60.875	-45.51
1		-7.244	-2.86	-0.433	-33.308	-5.494	-56.098	-38.803
2		-6.771	-2.796	-0.18	-46.483	-3.867	-65.492	-50.35
3		-6.664	-2.767	-0.171	-45.569	-4.042	-63.867	-49.611
4		-6.581	-2.544	-0.054	-42.874	-2.554	-60.835	-45.428
5		-6.546	-2.765	-0.167	-46.213	-3.094	-62.871	-49.307
6		-6.391	-2.75	-0.26	-39.714	-3.403	-57.906	-43.117

No.	Compound	Docking score (kcal/mol)	Glide lipo	Glide H bond interaction	Glide evdw interaction	Glide ecoul	Glide E-model	Glide Energy (kcal/mol)
7		-6.387	-2.507	-0.084	-43.624	-3.449	-61.029	-47.073
8		-6.372	-2.58	-0.354	-40.013	-3.581	-57.204	-43.594
9		-6.144	-2.619	-0.114	-43.684	-3.083	-60.001	-46.767
10		-6.14	-2.608	-0.252	-42.899	-1.897	-56.771	-44.796
11		-6.125	-2.515	-0.062	-45.449	-3.116	-62.115	-48.565
12		-6.121	-2.625	-0.134	-43.856	-3.033	-60.389	-46.889
13		-6.098	-2.679	-0.045	-45.35	-3.112	-62.162	-48.462
14		-6.082	-2.546	-0.2	-42.54	-3.669	-57.764	-46.209
15		-6.074	-2.813	-0.125	-45.566	-2.661	-58.884	-48.227
16		-5.988	-2.911	-0.371	-39.048	-4.32	-58.151	-43.369
17		-5.949	-2.604	-0.085	-43.007	-1.255	-57.16	-44.262
18		-5.939	-2.585	-0.364	-40.672	-4.692	-60.436	-45.364
19		-5.918	-2.552	-0.25	-44.172	-1.195	-59.664	-45.367
20		-5.892	-2.498	-0.169	-44.802	-1.914	-59.092	-46.716
21		-5.84	-2.923	0	-47.83	-3.57	-60.443	-51.4
22		-5.782	-2.541	-0.184	-43.578	-1.08	-54.15	-44.659
23		-5.773	-2.479	-0.012	-43.684	-1.912	-55.68	-45.596
24		-5.763	-2.623	-0.08	-44.044	-1.107	-57.647	-45.151

| No.	Compound	Docking score (kcal/mol)	Glide lipo	Glide H bond interaction	Glide evdw interaction	Glide ecoul	Glide E-model	Glide Energy (kcal/mol)
25		-5.742	-2.562	-0.205	-41.823	-1.106	-54.213	-42.929
26		-5.718	-1.679	-0.55	-37.788	-5.225	-56.404	-43.014
27		-5.697	-1.625	-0.498	-38.047	-6.16	-55.659	-44.207
28		-5.688	-2.625	-0.01	-45.641	0.583	-54.719	-45.058
29		-5.666	-2.629	-0.085	-43.871	-0.336	-56.134	-44.207
30		-5.66	-2.846	0	-42.935	-3.942	-64.186	-46.877
31		-5.646	-2.511	-0.213	-42.749	-3.178	-57.205	-45.927
32		-5.589	-2.603	0	-47.345	-1.081	-61.494	-48.426
33		-5.53	-2.513	-0.25	-44.582	-3.164	-58.862	-47.746
34		-5.509	-2.552	-0.149	-42.502	-2.842	-55.335	-45.344
35		-5.499	-2.882	-0.087	-42.499	-3.785	-57.444	-46.285
36		-5.49	-2.496	-0.162	-44.827	-4.581	-60.255	-49.408
37		-5.447	-2.403	-0.056	-46.198	-4.948	-61.352	-51.146
38		-5.427	-2.52	-0.192	-45.278	-2.9	-58.27	-48.178
39		-5.406	-2.539	-0.193	-45.532	-3.085	-58.687	-48.617
40		-5.401	-2.316	-0.16	-43.449	-3.757	-58.559	-47.206
41		-5.378	-2.519	0	-45.527	-2.827	-59.158	-48.354

| No.	Compound	Docking score (kcal/mol)	Glide lipo	Glide H bond interaction	Glide evdw interaction	Glide ecoul	Glide E-model	Glide Energy (kcal/mol)
42		-5.358	-2.508	-0.203	-45.49	-2.88	-58.207	-48.37
43		-5.342	-2.494	-0.16	-41.996	-2.6	-57.649	-44.596
44		-5.273	-2.658	-0.16	-41.803	-2.398	-56.083	-44.201
45		-5.236	-2.715	-0.116	-42.733	-2.43	-58.967	-45.163
46		-5.215	-2.542	0	-43.21	-2.644	-56.197	-45.854
47		-5.199	-2.35	-0.117	-42.463	-3.127	-53.193	-45.59
48		-5.156	-2.624	-0.073	-41.765	-3.164	-58.696	-44.929
49		-5.152	-2.41	-0.126	-41.545	-3.367	-57.37	-44.912
50		-5.118	-2.573	-0.125	-44.165	-1.269	-55.183	-45.434
51		-4.96	-2.492	-0.111	-43.037	-1.539	-52.005	-44.576

3.3 Molecular dynamic study.

A Molecular Dynamics (MD) Simulation was performed to understand the stability of the complex or drug molecule within the receptor. We conducted MD simulations for the molecules with the highest docking scores and standard molecules to compare Root Mean Square Deviation (RMSD) and Root Mean Square Fluctuation (RMSF). The simulations followed a well-established protocol, ensuring consistent conditions and parameters throughout the process. We selected the molecules with the highest docking scores and standard reference molecules to provide a comparative analysis. The average RMSD for all complexes ranged from 2.05 to 3.05 Å, indicating a high level of stability for the molecules throughout the MD simulation. The RMSD analyses confirmed that the Lck-benzothiazole complexes maintained stability during the entire MD simulation period. The RMSF graphs further supported the stability of these complexes, revealing that the N-terminal region had a higher fluctuation (~6.0 Å) compared to the C-terminal region (~2.5 Å). The lower fluctuation at the C-terminal suggests that this part of the complex remains more rigid and stable, which is crucial for maintaining the structural integrity of the molecule-receptor interaction. We also monitored non-bonded interactions of the ligands throughout the simulation, providing insights into how they interact with the receptor and maintain their positions, contributing to the overall stability. The combined analyses of RMSD, RMSF, and non-bond interactions demonstrate the robust

stability of the designed drug molecules within their respective receptors, validating their potential for enhanced anticancer profiles. The RMSD graphs depicted the stability and deviations over the simulation time (Figures 3a, 4a, 5a, 6a, 7a, 8a, 9a, 9b, and 9c), while the RMSF graphs illustrated the fluctuations in atomic positions, highlighting regions of stability and flexibility (Figures 3b, 4b, 5b, 6b, 7b, 8b, 10a, 10b, and 10c).
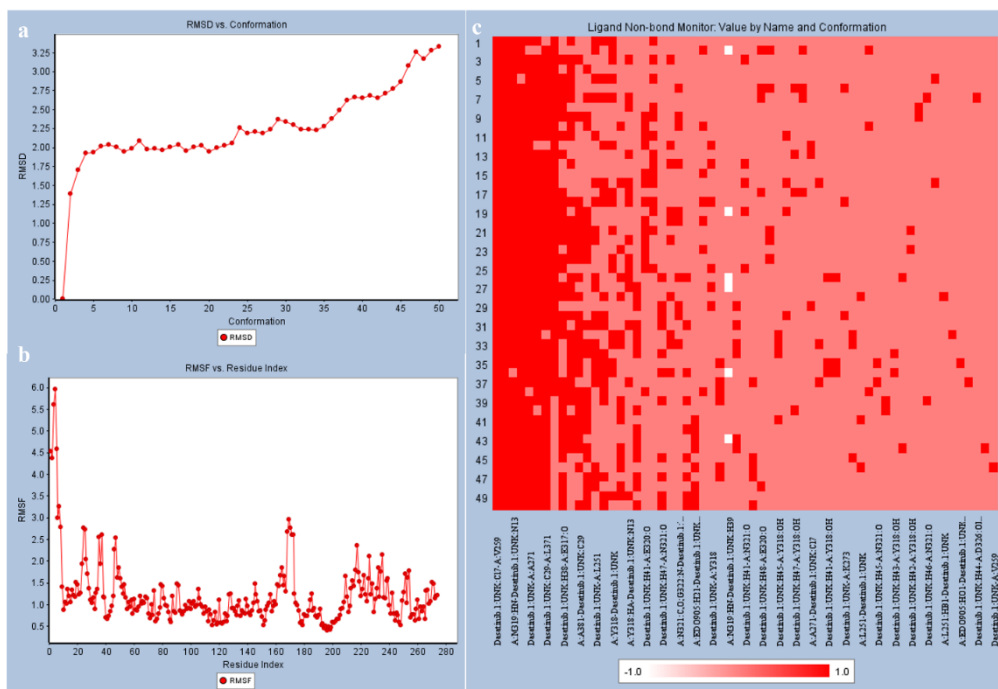
Figure 3. Result of molecular dynamics simulation **(a)** RMSD v/s Conformation graph of Dasatinib; **(b)** RMSF v/s Residual Index graph of Dasatinib; **(c)** Ligand Non-bond Monitor of Dasatinib.
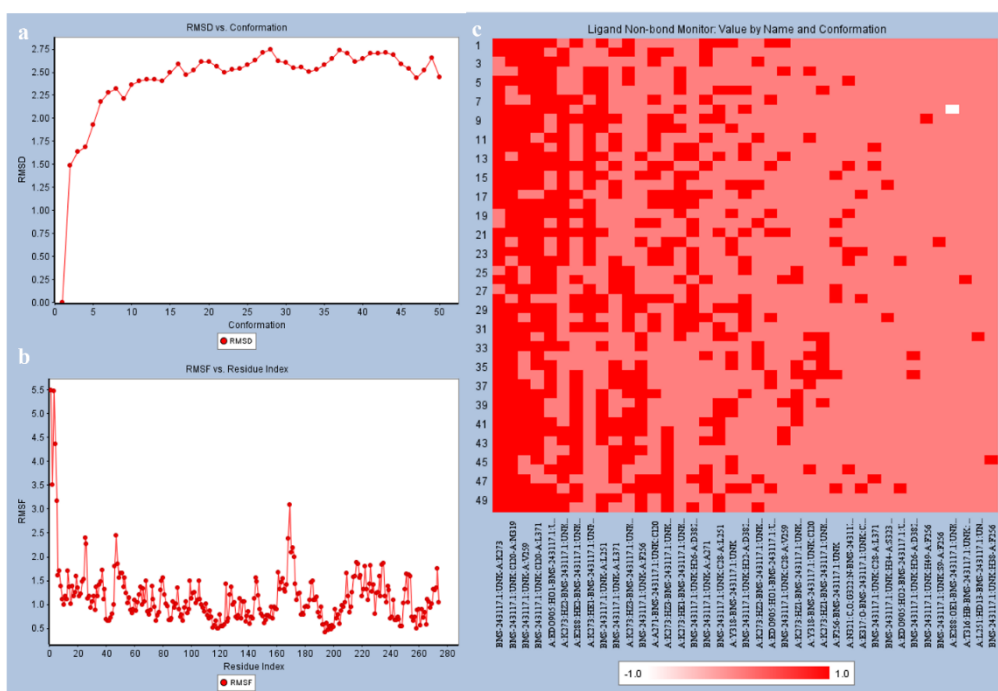
Figure 4. Result of molecular dynamics simulation **(a)** RMSD v/s Conformation graph of BMS-243117; **(b)** RMSF v/s Residual Index graph of BMS-243117; **(c)** Ligand Non-bond Monitor of BMS-243117.

The ligand non-bond monitor showed the interaction patterns between the ligands and receptor, supporting the stability findings (Figures 3c, 4c, 5c, 6c, 7c, and 8c). These comprehensive analyses provide a detailed understanding of the molecular stability and

interaction dynamics, ensuring the reliability of the designed molecules for further drug development.

Figure 5. Result of molecular dynamics simulation **(a)** RMSD v/s Conformation graph of 2-(Aminoheteroaryl)-thiazole-5-carboximide; **(b)** RMSF v/s Residual Index graph of 2-(Aminoheteroaryl)-thiazole-5-carboximide; **(c)** Ligand Non-bond Monitor of 2-(Aminoheteroaryl)-thiazole-5-carboximide.

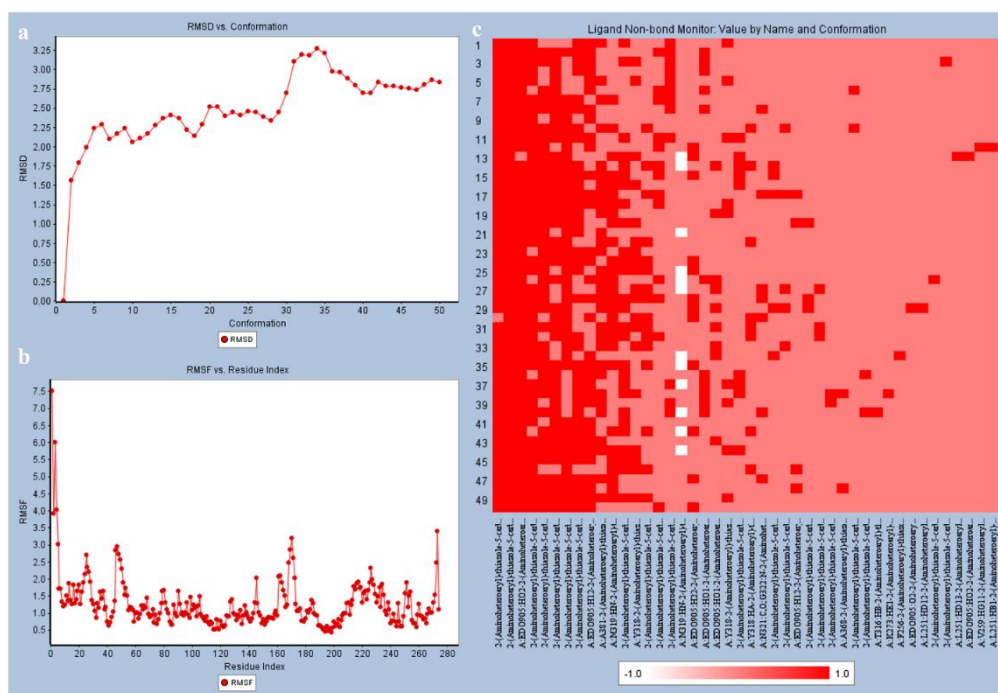**Figure 6.** Result of molecular dynamics simulation **(a)** RMSD v/s Conformation graph of Compound-1; **(b)** RMSF v/s Residual Index graph of Compound-1; **(c)** Ligand Non-bond Monitor of Compound-1.
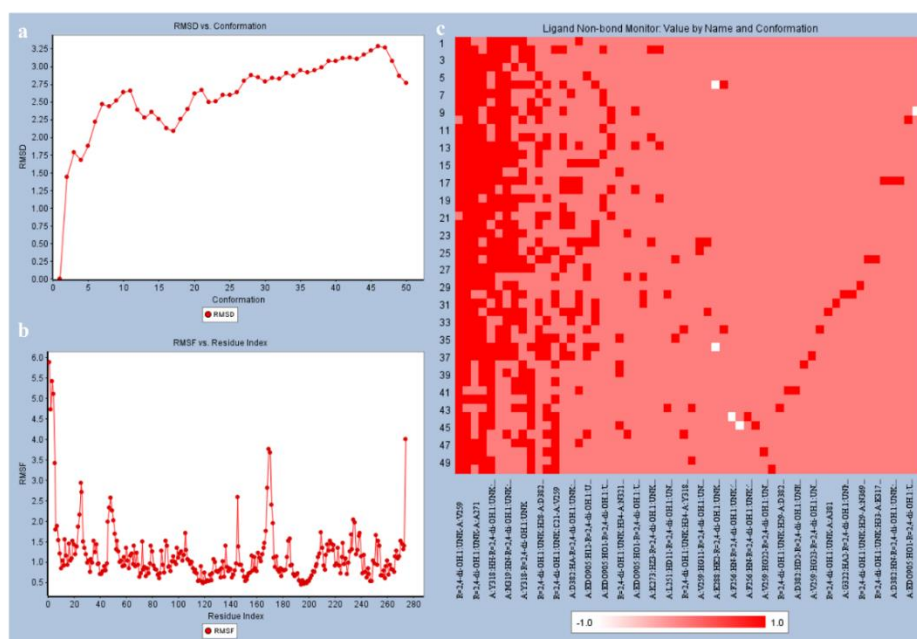
Figure 7. Result of molecular dynamics simulation **(a)** RMSD v/s Conformation graph of Compound-2; **(b)** RMSF v/s Residual Index graph of Compound-2; **(c)** Ligand Non-bond Monitor of Compound-2.
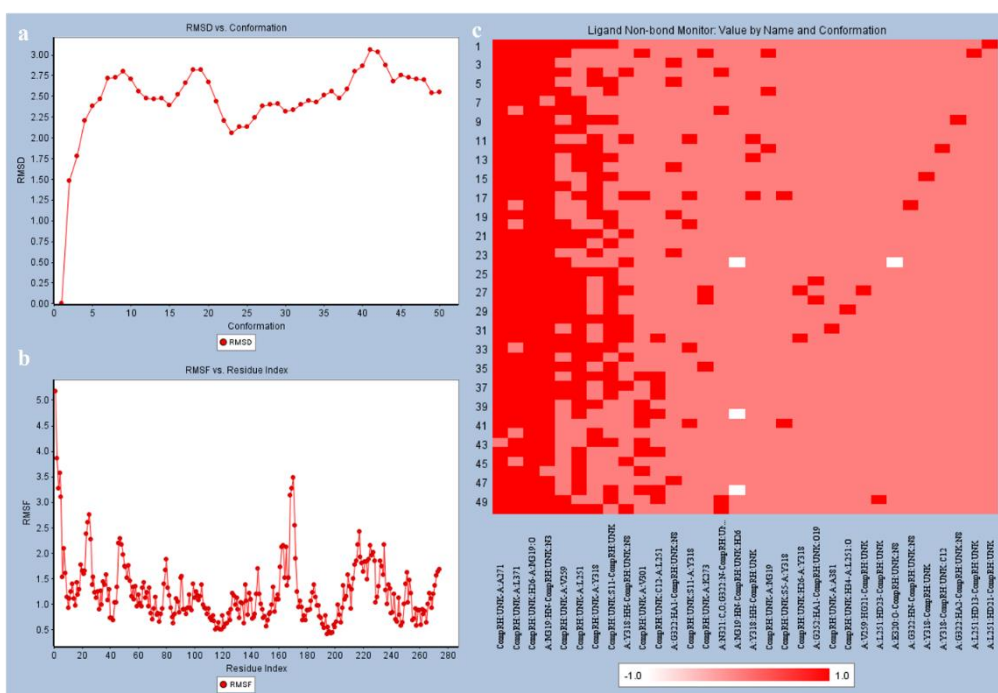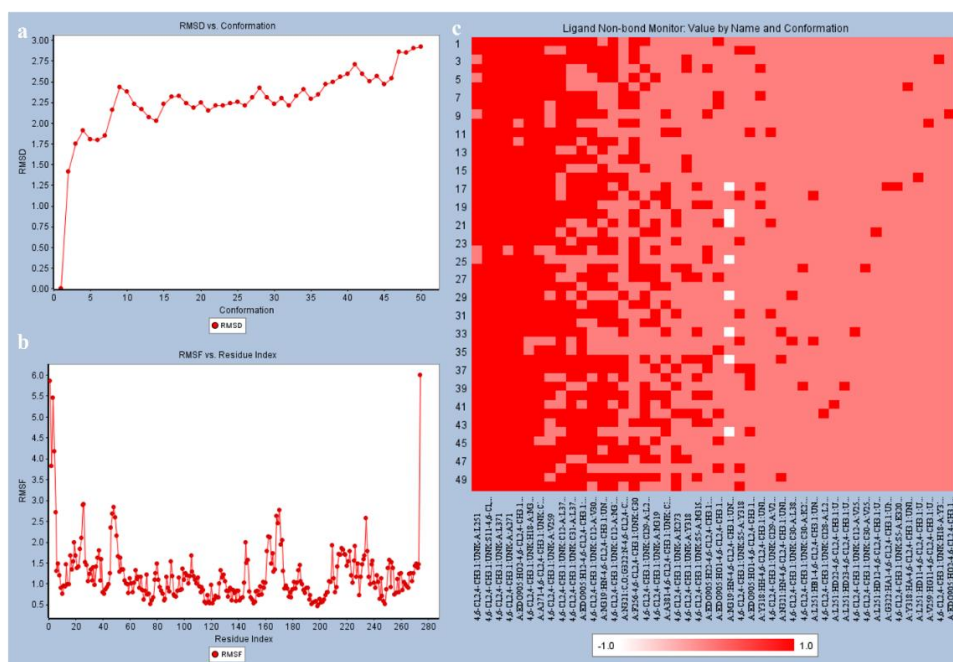

Figure 8. Result of molecular dynamics simulation **(a)** RMSD v/s Conformation graph of Compound-3; **(b)** RMSF v/s Residual Index graph of Compound-3; **(c)** Ligand Non-bond Monitor of Compound-3.

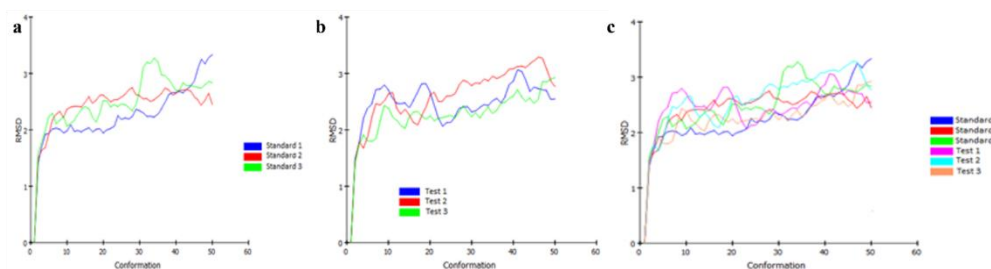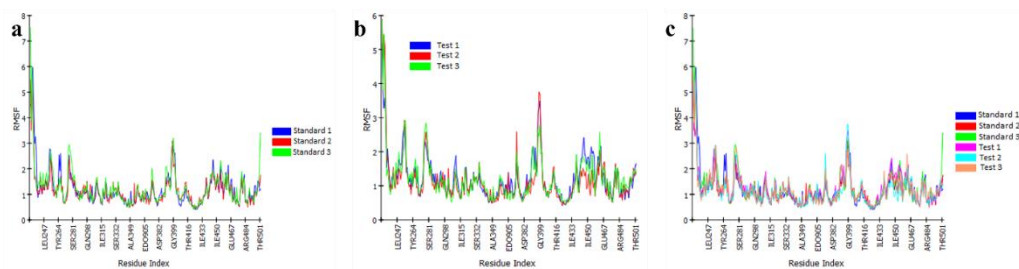
Figure 9. Result of molecular dynamics simulation **(a)** RMSD v/s Conformation graph of Standard Molecules; **(b)** RMSD V/S Conformation Graph of Test Molecules; **(c)** RMSD V/S Conformation Graph of Standard and Test Molecules.

Figure 10. Result of molecular dynamics simulation **(a)** RMSF V/S Residual Index of Standard Molecules; **(b)** RMSF V/S Residual Index of Test Molecules; **(c)** RMSF V/S Residual Index of Standard and Test Molecules.

4. Synthetic Feasibility for Designed Molecules

The designed molecules can be synthesized using a synthetic route, as per Figure 11. The ethyl acetoacetate reaction with thiourea gives 2-amino thiazole. Further, utilizing a free amino group with thiazole to react with various isothiocyanates gives thiourea derivatives, which further react with bromine for oxidative cyclization to give benzothiazole connected with thiazole through a secondary amine bridge. Further, the ester function on thiazole will be used to react with various anilines to give the final desired derivatives.
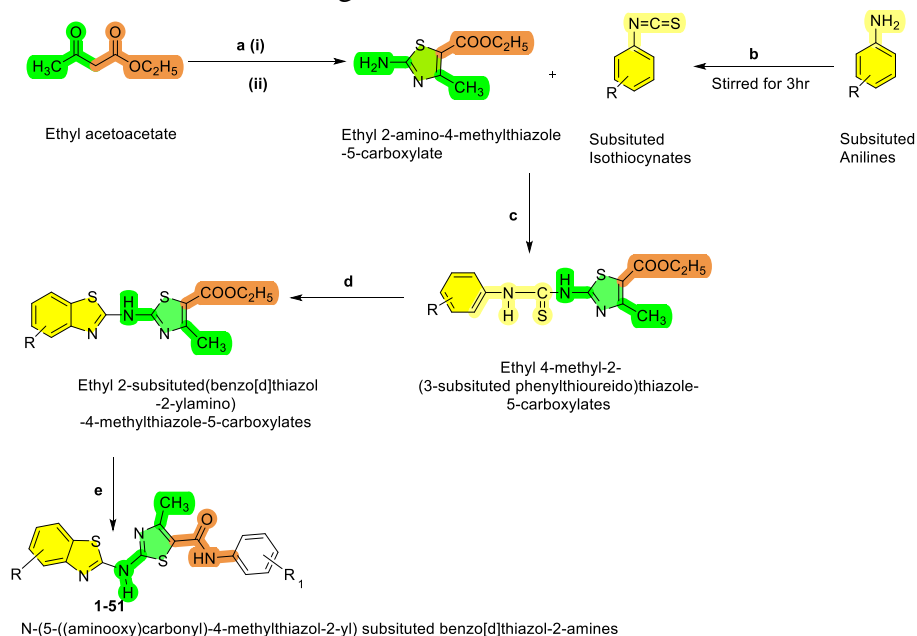
Figure 11. Route for synthesis of benzothiazole-thiazole hybrids **1-51;** Reagents **a)** (i) H_2O, NBS, THF, 0ºC (ii)Thiourea, 80ºC; **b)**$CSCl_2$, CH_2Cl_2; **c)** CH_3OH; **d)** $CHCl_3$; **e)** R´NH_2, KOt-Bu, THF.

5. Conclusions

The model was developed to predict the structural features of benzothiazoles to inhibit p56[lck], which shows useful information about the structural features required for the molecules. The molecular docking obtained helps us understand the structural features required by the ATP binding site of p56lck. The synthetic feasibility of designed benzothiazole-thiazole hybrids opens research for wet lab activity in vitro or in vivo, leading to LCK inhibition for cancer treatment. ADMET study results allowed us to determine the selectivity of substitution and to know whether molecules obey Lipinski's rule of five. Molecular docking study on designed molecules and some standard molecules gives information on binding patterns like hing region, Allosteric site, and activation loop.

Additionally, MD simulation studies on selected three molecules allowed us to understand the stability of the complex, ligand properties, and protein–ligand contacts. Altogether, these data suggest that compound 1 can potentially inhibit the p56[lck] enzyme. This work provides scope for further studies to establish the potential of benzothiazole derivatives as new p56[lck] inhibitors.

Funding

Acknowledgments

Conflict of Interest

The author(s) declare(s) that there is no conflict of interest regarding the publication of this article.

References

1. Sung, H.; Ferlay, J.; Siegel, R.L.; Laversanne, M.; Soerjomataram, I.; Jemal, A.; Bray, F. Global Cancer Statistics 2020: GLOBOCAN Estimates of Incidence and Mortality Worldwide for 36 Cancers in 185 Countries. *CA Cancer J. Clin.* **2021**, *71*, 209-249, http://doi.org/10.3322/caac.21660.
2. Jin, X.-Y.; Chen, H.; Li, D.-D.; Li, A.-L.; Wang, W.-Y.; Gu, W. Design, synthesis, and anticancer evaluation of novel quinoline derivatives of ursolic acid with hydrazide, oxadiazole, and thiadiazole moieties as potent MEK inhibitors. *J. Enzyme Inhib. Med. Chem.* **2019**, *34*, 955-972, http://doi.org/10.1080/14756366.2019.1605364.
3. Siegel, R.L.; Miller, K.D.; Fuchs, H.E.; Jemal, A. Cancer statistics, 2022. *CA Cancer J. Clin.* **2022**, *72*, 7-33, http://doi.org/10.3322/caac.21708.
4. Deo, S.V.S.; Sharma, J.; Kumar, S. GLOBOCAN 2020 Report on Global Cancer Burden: Challenges and Opportunities for Surgical Oncologists. *Ann. Surg. Oncol.* **2022**, *29*, 6497-6500, http://doi.org/10.1245/s10434-022-12151-6.
5. Kulothungan, V.; Sathishkumar, K.; Leburu, S.; Ramamoorthy, T.; Stephen, S.; Basavarajappa, D.; Tomy, N.; Mohan, R.; Menon, G.R.; Mathur, P. Burden of cancers in India-estimates of cancer crude incidence, YLLs, YLDs and DALYs for 2021 and 2025 based on National Cancer Registry Program. *BMC Cancer* **2022**, *22*, 527, http://doi.org/10.1186/s12885-022-09578-1.
6. Suma, V.R.; Sreenivasulu, R.; Rao, M.V.B.; Subramanyam, M.; Ahsan, M.J.; Alluri, R.; Rao, K.R.M. Design, synthesis, and biological evaluation of chalcone-linked thiazole-imidazopyridine derivatives as anticancer agents. *Med. Chem. Res.* **2020**, *29*, 1643-1654, http://doi.org/10.1007/s00044-020-02590-9.
7. Sayed, A.R.; Gomha, S.M.; Taher, E.A.; Muhammad, Z.A.; El-Seedi, H.R.; Gaber, H.M.; Ahmed, M.M. One-Pot Synthesis of Novel Thiazoles as Potential Anticancer Agents. *Drug des. devel. ther.* **2020**, *14*, 1363-1375, http://doi.org/10.2147/DDDT.S221263.
8. Bharatham, N.; Bharatham, K.; Lee, K.-W. P56 LCK Inhibitor Identification by Pharmacophore Modelling and Molecular Docking. *Bull. Korean Chem. Soc.* **2007**, *28*, 200-206, https://doi.org/10.5012/bkcs.2007.28.2.200.

9. Fassihi, A.; Sabet, R. QSAR Study of p56lck Protein Tyrosine Kinase Inhibitory Activity of Flavonoid Derivatives Using MLR and GA-PLS. *Int. J. Mol. Sci.* **2008**, *9*, 1876-1892, http://doi.org/10.3390/ijms9091876.

10. Badiger, A.M.; Noolvi, M.N.; Nayak, P.V. QSAR Study of Benzothiazole Derivatives as p56lck Inhibitors. *Lett. Drug Des. Discov.* **2006**, *3*, 550-560, http://doi.org/10.2174/157018006778194664.

11. Das, J.; Moquin, R.V.; Lin, J.; Liu, C.; Doweyko, A.M.; DeFex, H.F.; Fang, Q.; Pang, S.; Pitt, S.; Shen, D.R.; Schieven, G.L.; Barrish, J.C.; Wityak, J. Discovery of 2-amino-heteroaryl-benzothiazole-6-anilides as potent p56lck inhibitors. *Bioorg. Med. Chem. Lett.* **2003**, *13*, 2587-2590, http://doi.org/10.1016/S0960-894X(03)00511-0.

12. Das, J.; Chen, P.; Norris, D.; Padmanabha, R.; Lin, J.; Moquin, R.V.; Shen, Z.; Cook, L.S.; Doweyko, A.M.; Pitt, S.; Pang, S.; Shen, D.R.; Fang, Q.; de Fex, H.F.; McIntyre, K.W.; Shuster, D.J.; Gillooly, K.M.; Behnia, K.; Schieven, G.L.; Wityak, J.; Barrish, J.C. 2-Aminothiazole as a Novel Kinase Inhibitor Template. Structure− Activity Relationship Studies toward the Discovery of *N*-(2-Chloro-6-methylphenyl)-2-[[6-[4-(2-hydroxyethyl)-1-piperazinyl)]-2-methyl-4-pyrimidinyl]amino)]-1,3-thiazole-5-carboxamide (Dasatinib, BMS-354825) as a Potent *pan*-Src Kinase Inhibitor. *J. Med. Chem.* **2006**, *49*, 6819-6832, https://doi.org/10.1021/jm060727j.

13. Das, J.; Lin, J.; Moquin, R.V.; Shen, Z.; Spergel, S.H.; Wityak, J.; Doweyko, A.M.; DeFex, H.F.; Fang, Q.; Pang, S.; Pitt, S.; Shen, D.R.; Schieven, G.L.; Barrish, J.C. Molecular design, synthesis, and structure–Activity relationships leading to the potent and selective p56[lck] inhibitor BMS-243117. *Bioorg. Med. Chem. Lett.* **2003**, *13*, 2145-2149, http://doi.org/10.1016/S0960-894X(03)00380-9.

14. Broadbridge, R.J.; Sharma, R.P. The Src Homology-2 Domains (SH2 Domains) of the Protein Tyrosine Kinase p56 lck Structure, Mechanism and Drug Design. *Curr. Drug Targets* **2000**, *1*, 365-386, http://doi.org/10.2174/1389450003349074.

15. Huang, S.; Liu, Z.; Tian, S.-S.; Sandberg, M.; Spalding, T.A.; Romeo, R.; Iskandar, M.; Wang, Z.; Karanewsky, D.; He, Y. Discovery of 2-amino-6-carboxamidobenzothiazoles as potent Lck inhibitors. *Bioorg. Med. Chem. Lett.* **2008**, *18*, 2324-2328, http://doi.org/10.1016/j.bmcl.2008.02.079.

16. Zhu, X.; Kim, J.L.; Newcomb, J.R.; Rose, P.E.; Stover, D.R.; Toledo, L.M.; Zhao, H.; Morgenstern, K.A. Structural analysis of the lymphocyte-specific kinase Lck in complex with non-selective and Src family selective kinase inhibitors. *Structure* **1999,** *7*, 651-661, https://doi.org/10.1016/S0969-2126(99)80086-0.

17. Yamaguchi, H.; Hendrickson, W.A. Structural basis for activation of human lymphocyte kinase Lck upon tyrosine phosphorylation. *Nature* **1996**, *384*, 484-489, http://doi.org/10.1038/384484a0.

18. Snow, R.J.; Cardozo, M.G.; Morwick, T.M.; Busacca, C.A.; Dong, Y.; Eckner, R.J.; Jacober, S.; Jakes, S.; Kapadia, S.; Lukas, S.; Panzenbeck, M.; Peet, G.W.; Peterson, J.D.; Prokopowicz, A.S.; Sellati, R.; Tolbert, R.T.; Tschantz, M.A.; Moss, N. Discovery of 2- Phenylamino-imidazo[4,5-*h*]isoquinolin-9-ones: A New Class of Inhibitors of Lck Kinase. *J. Med. Chem.* **2002**, *45*, 3394-3405, http://doi.org/10.1021/jm020113o.

19. Khatik, R.; Pathak, A.K. LcK Inhibitors and its analogues: A Review. *Der. Pharma. Chem.* **2011**, *3*, 310-320.

20. Meyn III, M.A.; Smithgall, T.E. Small Molecule Inhibitors of Lck: The Search for Specificity within a Kinase Family. *Mini Rev. Med. Chem.* **2008**, *8*, 628-637, http://doi.org/10.2174/138955708784534454.

21. Bommhardt, U.; Schraven, B.; Simeoni, L. Beyond TCR Signaling: Emerging Functions of Lck in Cancer and Immunotherapy. *Int. J. Mol. Sci.* **2019**, *20*, 3500, http://doi.org/10.3390/ijms20143500.

22. Warmuth, M.; Damoiseaux, R.; Liu, Y.; Fabbro, D.; Gray, N. SRC Family Kinases: Potential Targets for the Treatment of Human Cancer and Leukemia. *Curr. Pharm. Des.* **2003**, *9*, 2043-2059, http://doi.org/10.2174/1381612033454126.

23. Won, J.; Lee, G.H. T-Cell–Targeted Signaling Inhibitors. *Int. Rev. Immunol.* **2008**, *27*, 19-41, http://doi.org/10.1080/08830180701798976.

24. Zhang, J.; Yang, P.L.; Gray, N.S. Targeting cancer with small molecule kinase inhibitors. *Nat. Rev. Cancer* **2009**, *9*, 28-39, http://doi.org/10.1038/nrc2559.

25. Avvaru, S.P.; Noolvi M.N.; More U.A.; Chakraborty S.; Dash A.; Aminabhavi T.M.; Narayan K.P; Sutariya V. Synthesis and anticancer activity of thiadiazole containing thiourea, benzothiazole and imidazo [2, 1-b][1, 3, 4] thiadiazole scaffolds. Medicinal Chemistry. **2021** Aug 1;17(7):750-65

26. Balanean, L.; Braicu, C.; Berindan-Neagoe, I.; Nastasa, C.M.; Tiperciuc, B.; Verite, P.; Oniga, O. Synthesis of Novel 2-metylamino-4-substituted-1,3-thiazoles with Antiproliferative Activity. *Rev. de Chim.* **2014**, *65*, 1413-1417.

27. Davyt, D.; Serra, G. Thiazole and Oxazole Alkaloids: Isolation and Synthesis. *Mar. Drugs* **2010**, *8*, 2755-2780, http://doi.org/10.3390/md8112755.

28. Tsai, C.-Y.; Kapoor, M.; Huang, Y.-P.; Lin, H.-H.; Liang, Y.-C.; Lin, Y.-L.; Huang, S.-C.; Liao, W.-N.; Chen, J.-K.; Huang, J.-S.; Hsu, M.-H. Synthesis and Evaluation of Aminothiazole-Paeonol Derivatives as Potential Anticancer Agents. *Molecules* **2016**, *21*, 145, http://doi.org/10.3390/molecules21020145.

29. Cai, W.-X.; Liu, A.-L.; Li, Z.-M.; Dong, W.-L.; Liu, X.-H.; Sun, N.-B. Synthesis and Anticancer Activity of Novel Thiazole-5-Carboxamide Derivatives. *Appl. Sci.* **2016**, *6*, 8, http://doi.org/10.3390/app6010008.

30. Siddiqui, N.; Arya, S.K.; Ahsan, W.; Azad, B. Diverse biological activities of Thiazoles: A Retrospect. *Int. J. Drug Dev. Res.* **2011**, *3*, 56-67.

31. Pinninti, S.K.; Parimi, U. SYNTHESIS AND BIOLOGICAL EVALUATION OF AMIDE DERIVATIVES OF THIAZOLES AND ANTICANCER AGENTS. *Int. Res. J. Pharm.* **2018**, *9*, 89-93.

32. Altıntop, M.D.; Sever, B.; Akalın Çiftçi, G.; Özdemir, A. Design, Synthesis, and Evaluation of a New Series of Thiazole-Based Anticancer Agents as Potent Akt Inhibitors. *Molecules* **2018**, *23*, 1318, http://doi.org/10.3390/molecules23061318.

33. Radwan, A.S.; Khalid, M.A.A. Synthesis, Docking, and Anticancer Activity of New Thiazole Clubbed Thiophene, Pyridine, or Chromene Scaffolds. *J. Heterocycl. Chem.* **2019**, *56*, 1063-1074, http://doi.org/10.1002/jhet.3493.

34. Abdel-Sattar, N.E.A.; El-Naggar, A.M.; Abdel-Mottaleb, M.S.A. Novel Thiazole Derivatives of Medicinal Potential: Synthesis and Modeling. *J. Chem.* **2017**, *2017*, 4102796, http://doi.org/10.1155/2017/4102796.

35. Zhang, Z.-H.; Wu, H.-M.; Deng, S.-N.; Cai, X.-Y.; Yao, Y.; Mwenda, M.C.; Wang, J.-Y.; Cai, D.; Chen, Y. Design, Synthesis, and Anticancer Activities of Novel 2-Amino-4-phenylthiazole Scaffold Containing Amide Moieties. *J. Chem.* **2018**, *2018,* 4301910, https://doi.org/10.1155/2018/4301910.

36. Alizadeh, S.R.; Hashemi, S.M., Development and therapeutic potential of 2-aminothiazole derivatives in anticancer drug discovery. *Med. Chem. Res.* **2021**, *30*, 771-806, https://doi.org/10.1007/s00044-020-02686-2.

37. Thakur, S.; Sharma, R.; Yadav, R.; Sardana, S. The Potential of Thiazole Derivatives as Antimicrobial Agents. *Chem. Proc.* **2022,** *12*, 36, http://doi.org/10.3390/ecsoc-26-13673.

38. Chahal, S.; Punia, J.; Rani, P.; Singh, R.; Mayank; Kumar, P.; Kataria, R.; Joshi, G.; Sindhu, J. Development of thiazole-appended novel hydrazones as a new class of α-amylase inhibitors with anticancer assets: an *in silico* and *in vitro* approach. *RSC Med. Chem.* **2023**, *14,* 757-781, http://doi.org/10.1039/D2MD00431C.

39. Ayman, M.; Abdelmonsef, A.H.; Rashdan, H.R.M. Mini Review on The Synthesis and Biological Impact of Thiazoles. *ChemistrySelect* **2023**, *8*, e202300414, https://doi.org/10.1002/slct.202300414.

40. Swathykrishna, C.S.; Amrithanjali, G.; Shaji, G.; Kumar A.R. Antimicrobial Activity and Synthesis of Thiazole Derivatives: A Recent Update. *J. Chem. Rev.* **2023**, *5*, 221-240, https://doi.org/10.22034/JCR.2023.383674.1211.

41. Shahin, I.G.; Mohamed, K.O.; Taher, A.T.; Mayhoub, A.S.; Kassab A.E. Recent Advances in the Synthesis of Thiazole Ring: Mini Review. *Mini-Rev. Org. Chem.* **2023**, *20,* 270-284, https://doi.org/10.2174/1570193X19666220413104255.

42. Haider, K.; Shrivastava, N.; Pathak, A.; Dewangan, R.P.; Yahya, S.; Yar, M.S. Recent advances and SAR study of 2-substituted benzothiazole scaffold based potent chemotherapeutic agents. *Results Chem.* **2022**, *4*, 100258, https://doi.org/10.1016/j.rechem.2021.100258.

43. Kemisetti, D.; Amin, R.; Alam, F.; Gacem, A.; Emran, T.B.; Alsufyani, T.; Alqahtani, M.S.; Islam, S.; Matin, M.M.; Jameel, M. Novel Benzothiazole Derivatives Synthesis and its Analysis as Diuretic Agents. *Evid. Based Complementary Altern. Med.* **2023**, *2023*, 5460563, https://doi.org/10.1155/2023/5460563.

44. Racané, L.; Pavelić, S.K.; Ratkaj, I.; Stepanić, V.; Pavelić, K.; Tralić-Kulenović, V.; Karminski-Zamola, G. Synthesis and antiproliferative evaluation of some new amidino-substituted bis-benzothiazolyl-pyridines and pyrazine. *Eur. J. Med. Chem.* **2012**, *55*, 108-116, http://doi.org/10.1016/j.ejmech.2012.07.005.

45. Patel, N.B.; Khan, I.H. Synthesis of 1,2,4-triazole derivatives containing benzothiazoles as pharmacologically active molecule. *J. Enzyme Inhib. Med. Chem.* **2011**, *26*, 527-534, http://doi.org/10.3109/14756366.2010.535794.

46. Wongso, H.; Ono, M.; Yamasaki, T.; Kumata, K.; Higuchi, M.; Zhang, M.-R.; Fulham, M.J.; Katsifis, A.; Keller, P.A. Synthesis and structure–activity relationship (SAR) studies of 1,2,3-triazole, amide, and ester-based benzothiazole derivatives as potential molecular probes for tau protein. *RSC Med. Chem.* **2023**, *14,* 858-868, http://doi.org/10.1039/D2MD00358A.

47. Mendieta-Wejebe, J.E.; Rosales-Hernández, M.C.; Padilla-Martínez I.I.; García-Báez, E.V.; Cruz, A. Design, Synthesis and Biological Activities of (Thio)Urea Benzothiazole Derivatives. *Int. J. Mol. Sci.* **2023**, *24*, 9488, https://doi.org/10.3390/ijms24119488.

48. Lihumis, H.S.; Alameri, A.A.; Zaooli, R.H. A Review on Recent Development and biological applications of benzothiazole derivatives. *Prog. Chem. Biochem. Res.* **2022**, *5,* 147-164, http://doi.org/10.22034/pcbr.2022.330703.1214.

49. Catalano, A.; Carocci, A.; Defrenza, I.; Muraglia, M.; Carrieri, A.; Van Bambeke, F.; Rosato, A.; Corbo, F.; Franchini, C. 2-Aminobenzothiazole derivatives: Search for new antifungal agents. *Eur. J. Med. Chem.* **2013**, *64*, 357-364, http://doi.org/10.1016/j.ejmech.2013.03.064.

50. Kumar, S.; Dubey, B. A Review on Emerging Benzothiazoles: Biological Aspects. *J. Drug. Deliv. Ther.* **2022**, *12*, 270-274, https://doi.org/10.22270/jddt.v12i4-S.5549.

51. Chauhan, B.; Kumar, R.; Salahuddin; Singh, H.; Afzal, O.; Altamimi, A.S.A.; Abdullah, M.M.; Yar, M.S.; Ahsan, M.J.; Kumar, N.; Yadav, S.K. Design, Synthesis, *In Vivo*, and *In Silico* Evaluation of Benzothiazoles Bearing a 1,3,4-Oxadiazole Moiety as New Antiepileptic Agents. *ACS Omega* **2023**, *8*, 2520-2630, https://doi.org/10.1021/acsomega.2c06967.

52. Gupta, K.; Sirbaiya, A.K.; Kumar, V.; Rahman, M.A. Current Perspective of Synthesis of Medicinally Relevant Benzothiazole based Molecules: Potential for Antimicrobial and Anti-Inflammatory Activities. *Mini. Rev. Med. Chem.* **2022**, *22*, 1895-1935, https://doi.org/10.2174/1389557522666220217101805.

53. Kumar, M.N.; Nukala, S.K.; Swamy, N.T.; Ravinder, M.; Krishna, T.M.; Narsimha, S. Benzothiazole-[1,2,3]triazolo[5,1-a]isoindoles: Synthesis, anticancer activity, bioavailability and in silico studies against Gama-Tubulin protein. *J. Mol. Struct.* **2022**, *1250*, 131722, https://doi.org/10.1016/j.molstruc.2021.131722.

54. Li, B.; Liu, Y.; Uno, T.; Gray, N. Creating chemical diversity to target protein kinases. *Comb. Chem. High Throughput Screen* **2004**, *7*, 453-472, https://doi.org/10.2174/1386207043328580.

55. Glide, Schrödinger, LLC, New York, NY, 2017.

56. Accelrys Discovery Studio, release 3.0, Accelrys Inc., San Diego, CA.

57. Ryckaert, J.-P.; Ciccotti, G.; Berendsen, H.J.C. Numerical integration of the cartesian equations of motion of a system with constraints: molecular dynamics of n-alkanes. *J. Comput. Phys.* **1977**, *23*, 327-341, https://doi.org/10.1016/0021-9991(77)90098-5.

58. Brooks, B.R.; Brooks III, C.L.; Mackerell Jr., A.D.; Nilsson, L.; Petrella, R.J.; Roux, B.; Won, Y.; Archontis, G.; Bartels, C.; Boresch, S.; Caflisch, A.; Caves, L.; Cui, Q.; Dinner, A.R.; Feig, M.; Fischer, S.; Gao, J.; Hodoscek, M.; Im, W.; Kuczera, K.; Lazaridis, T.; Ma, J.; Ovchinnikov, V.; Paci, E.; Pastor, R.W.; Post, C.B.; Pu, J.Z.; Schaefer, M.; Tidor, B.; Venable, R.M.; Woodcock, H.L.; Wu, X.; Yang, W.; York, D.M.; Karplus, M. CHARMM: The biomolecular simulation program. *J. Comput. Chem.* **2009**, *30*, 1545-1614, https://doi.org/10.1002/jcc.21287.